HHS Public Access

Author manuscript

Cell Stem Cell. Author manuscript; available in PMC 2017 December 01.

Published in final edited form as:

Cell Stem Cell. 2016 December 01; 19(6): 738–751. doi:10.1016/j.stem.2016.09.002.

Skin adipocyte stem cell self-renewal is regulated by a Pdgfa/Akt signaling axis

Guillermo C. Rivera-Gonzalez[1], **Brett A. Shook**[1], **Johanna Andrae**[4], **Brandon Holtrup**[3], **Katherine Bollag**[1], **Christer Betsholtz**[4], **Matthew S. Rodeheffer**[1,3], and **Valerie Horsley**[1,2,5]

[1]Yale University, Department of Molecular, Cellular and Developmental Biology, New Haven, Connecticut 06520, USA

[2]Yale School of Medicine, Department of Dermatology, New Haven, Connecticut 06520, USA

[3]Section of Comparative Medicine, New Haven, Connecticut 06520, USA

[4]Uppsala University, Department of Immunology, Genetics and Pathology, Rudbeck Laboratory Uppsala 751 85, Sweden

Summary

Tissue growth and maintenance requires stem cell populations that self-renew, proliferate and differentiate. Maintenance of white adipose tissue (WAT) requires the proliferation and differentiation of adipocyte stem cells (ASCs) to form postmitotic, lipid-filled mature adipocytes. Here, we use the dynamic adipogenic program that occurs during hair growth to uncover an unrecognized regulator of ASC self-renewal and proliferation, Pdgfa, which activates Akt signaling to drive and maintain the adipogenic program in the skin. *Pdgfa* expression is reduced in aged ASCs and is required for ASC proliferation and maintenance in the dermis but not in other WATs. Our molecular and genetic studies uncover PI3K/Akt2 as a direct Pdgfa target, activated in ASCs during WAT hyperplasia and functionally required for dermal ASC proliferation. Our data therefore reveal active mechanisms that regulate ASC self-renewal in the skin and show that distinct regulatory mechanisms operate in different WAT depots.

Graphical Abstract

Correspondence should be addressed to: Valerie Horsley, valerie.horsley@yale.edu, Dept. of Molecular, Cellular and Developmental Biology, Yale University, 219 Prospect St., Box 208103, New Haven, CT 06520, Tel #203-436-9126, Fax #203-432-6161.
[5]Lead Contact

Author contributions

G.C.R-G. and V.H. designed the experiments. G.C.R-G., B.A.S., B.H. and K.B. performed the experiments and analyzed the data. G.C.R-G., B.A.S., M.S.R and V.H. discussed and interpreted the analyses. J.A. and C.B. provided the *Pdgfa*^{fl} mice and interpreted the analyses. The manuscript was written by G.C.R-G. and V.H and edited by all authors.

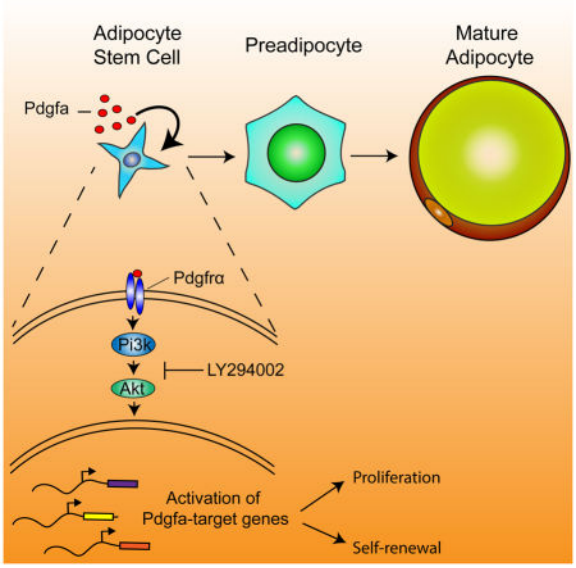

Keywords

Adipocyte stem cells; self-renewal; Pdgfa; PI3K/Akt signaling; skin

Introduction

Adult tissue homeostasis and expansion requires proliferation and differentiation of precursor cells to maintain stem cell (SC) pools and renew tissue specific cells (Pellettieri and Sánchez Alvarado, 2007). While adult SCs of many tissues have been identified and the mechanisms by which they are regulated are becoming increasingly understood (Adam et al., 2015; Beerman and Rossi, 2015; Donati and Watt, 2015; Goodell et al., 2015), the regulation of SCs within white adipose tissue (WAT) is not well understood. Because mature adipocytes are post-mitotic (Freytag, 1988; Shugart and Umek, 1997), new adipocytes arise from the proliferation and differentiation of adipocyte precursor (AP) cells residing within adipose tissue (Cristancho and Lazar, 2011; Rodeheffer et al., 2008). Indeed, we and others identified AP cells within several depots of WAT in mice including the traditional visceral (vWAT), subcutaneous (sWAT) depots, as well as in the skin's dermis (dWAT) (Berry and Rodeheffer, 2013; Festa et al., 2011; Rodeheffer et al., 2008). Recent studies have shown that AP cells can be regulated in a depot specific-manner (Jeffery et al., 2015; 2016; Wang et al., 2013). However, the molecular cues regulating AP maintenance, activation and differentiation in the myriad of *in vivo* contexts remain largely unknown.

The skin provides an excellent model to study the regulation of adipogenesis and AP maintenance. dWAT is a major component of the skin's dermal thickness (Chase et al., 1953) and undergoes rounds of dramatic regression and expansion in response to hair regeneration and also expands following bacterial infection and cold stress (Festa et al., 2011; Hansen et al., 1984; Kasza et al., 2014; Zhang et al., 2015). Rapid growth and regression of dWAT can occur in a few days whereas vWAT and sWAT display relatively

slow turnover during tissue maintenance and there is minimal expansion of these depots during obesity (Arner et al., 2013; Cleary et al., 1979; Faust et al., 1978; Jeffery et al., 2015; Lemonnier, 1972; Spalding et al., 2008; Wang et al., 2013), making the skin a robust model for defining adipose regulatory mechanisms.

Here, using genetic lineage tracing and *in vivo* AP proliferation assays, we show that hyperplasia of dWAT occurs during hair regeneration and is preceded by proliferation of a distinct population of adipocyte stem cells (ASCs) that we previously identified as CD24+ ASCs. We demonstrate that CD24+ ASCs are lost when dWAT mass is reduced after multiple hair cycles, both in the context of aging and depilation. Using conditional deletion of *Pdgfa* and competitive transplantation of *Pdgfra* null APs in mice, we show that Pdgfa expression by dermal mesenchymal cells maintains CD24+ ASCs and dWAT mass. Employing gene expression analysis, functional *in vitro* and *in vivo* activation assays and genetic depletion mouse models, we identify genetic targets and a PI3K/Akt signaling axis downstream of Pdgfa in the regulation of dermal CD24+ ASCs.

Results

Defining adipocyte hyperplasia in the skin

One of the remarkable changes that occurs in the skin during hair growth is the expansion of dWAT (Donati et al., 2014; Festa et al., 2011). To quantitatively assess the formation of new adipocytes during the hair follicle cycle, we performed a pulse-chase experiment to label mature adipocytes using the adipocyte-specific, tamoxifen inducible *Adiponectin*-Cre Estrogen Receptor (*Adiponectin*-CreER) mouse model (Jeffery et al., 2014) in combination with a dual fluorescent reporter. Upon activation of Cre recombinase activity, the fluorescent reporter undergoes an irreversible switch from expression of plasma membrane-targeted Tomato (mT) to plasma membrane-targeted GFP expression (mG, green fluorescence) allowing robust identification of Cre-expressing cells (Berry and Rodeheffer, 2013; Muzumdar et al., 2007) (Figure 1A). Tamoxifen treatment of *Adiponectin*-CreER;mT/mG mice resulted in 96% recombination efficiency in intradermal adipocytes (Figures 1B–C). To observe the formation of new adipocytes, we pulsed *Adiponectin*-CreER;mT/mG mice with tamoxifen from P18–P19, when hair follicles are regressing. We then analysed the labelling of adipocytes during rest stage of the hair follicle cycle (telogen, P20) and after endogenous induction of the first round of hair regeneration (anagen, P34)(Figure 1A). Since the mTomato signal was weak in frozen skin sections, we immunostained skin sections with antibodies against perilipin to delineate the lipid droplet within mature adipocytes. By quantifying the percentage of perilipin+ adipocytes that were GFP- at P34, we observed ~20% of adipocytes are generated *de novo* in dWAT during hair growth (Figures 1B and 1C).

Recently, we identified two subpopulations of Sca1+ APs in vWAT and sWAT, including CD24+ ASCs that give rise to CD24− preadipocytes (Berry and Rodeheffer, 2013; Rodeheffer et al., 2008). FACS analysis of AP cells revealed CD24+ ASC and CD24− preadipocyte cells in the dermis (Figure 1D and S1) and showed an increase in both AP populations during hair follicle growth (Figure 1E). CD24+ ASCs increase progressively during hair growth, whereas CD24− preadipocyte numbers peak immediately prior to hair

follicle SC activation. To determine if differences in AP cell numbers reflect alterations in proliferation, we pulsed mice with EdU for 6 hrs at several time points prior to and after hair follicle growth. CD24+ ASCs proliferated significantly more than CD24− preadipocytes before hair growth activation (P16–18) with the proliferation rates peaking at P18 during dWAT regression and prior to hair follicle stem cell activation at P21 (Figures 1F–G). These data are consistent with the robust proliferation in CD24+ ASCs in vWAT in response to high fat diet feeding (Jeffery et al., 2015) and demonstrates that CD24+ ASCs display dynamic activation during the hair cycle.

Immature and mature adipocytes are depleted with age and hair depilation

Age-related changes to the skin include thinning of the dermis (Luo et al., 2002; Sun et al., 2004; Tchkonia et al., 2010; Tyner et al., 2002), which coincides with a decrease in dWAT and an increase in the papillary and reticular dermis (Figures 2A–D). To evaluate whether loss of CD24+ ASCs might contribute to the degeneration of dWAT in aged mice, we analysed CD24+ ASCs and CD24− preadipocytes in the skin of young (3 weeks old) and aged (18, 24 and 30 month-old) mice using FACS. The fraction of CD24+ ASCs were preferentially lost during aging, reduced by approximately 50% (Figures 2E–G), suggesting that age predominantly impacts CD24+ ASC maintenance.

Recent work demonstrated that multiple rounds of hair depilation induce serial cycles of hair growth and reduced the numbers of hair follicle stem cells (Keyes et al., 2013). To determine if repeated depilation alters dWAT and adipogenic lineage cells, we analysed dWAT after a single depilation or after 3 rounds of depilation. Similar to alterations of the dermis with age, serial depilation led to a significant reduction of dWAT area and mature adipocyte numbers compared to a single round of depilation (Figures 2H–J). Multiple rounds of depilation also reduced the percentage and proliferation of CD24+ ASCs and CD24− preadipocytes with CD24+ ASCs displaying a more dramatic reduction (Figures 2K–M and S2A–B). Together, these data indicate that CD24+ ASCs are differentially regulated compared to CD24− preadipocytes during hair cycling and with age.

Pdgfa is neccesary to maintain CD24+ ASCs and dWAT

We previously showed that *Pdgfa* and its receptor *Pdgfrα* are expressed by APs (Berry and Rodeheffer, 2013; Festa et al., 2011). Analysis of *Pdgfa* expression in CD24+ ASCs and CD24− preadipocytes showed that *Pdgfa* levels are significantly elevated between P16–18 (Figure 3A) when CD24+ ASCs are proliferative (Figure 1F–G) and significantly decrease by P32 (Figure 3A). While *Pdgfa* expression in CD24+ ASCs is not altered during depilation (Figure S2C–E), *Pdgfa* and *Pdgfrα* mRNA levels in AP cells from 3 week, 18 month and 30 month old mice revealed a significant downregulation with age when CD24+ ASCs maintenance is reduced (Figure 3B and 2E–G).

To investigate the role of *Pdgfa* in maintaining APs in the skin, we deleted *Pdgfa* in dermal mesenchymal cells by crossing mice expressing Cre recombinase driven by the *Pdgfrα* promoter with $Pdgfa^{fl}$ mice (*Pdgfa* cKO) (Andrae et al., 2014). The floxed *Pdgfa* allele introduces *LacZ* into exon 4, creating a truncated, biologically inactive protein (Figure S3A) (Andrae et al., 2014). During hair regression and rest (telogen), dWAT area and adipocyte

numbers were not different between WT and *Pdgfa* cKO mice (Figure S3B–D). However, upon hair follicle growth, the expansion of dWAT was attenuated in *Pdgfa* cKO (Figure 3C) as demonstrated by a significant reduction in dWAT area and a ~20% reduction in mature intradermal adipocytes in *Pdgfa* cKO mice (Figures 3D–E). Since 20% of adipocytes are generated de novo during the first hair cycle (Figure 1C) and since ASCs generate mature adipocytes (Festa, Ryan, and Jeffery), these data reveal that the adipogenic program is diminished in the dermis of *Pdgfa* cKO mice.

Since Pdgfa has been suggested to play a role in regulating the hair follicle cycle (Karlsson et al., 1999), we investigated whether hair cycling defects occurred in *Pdgfa* cKO mice to impact adipocyte regeneration. Hair regression and regrowth occurred with similar timing in *Pdgfa* cKO mice and WT mice during the first hair cycle (Figure S3E–H). Since Pdgf family members have overlapping roles (Chen et al., 2004; Donovan et al., 2013), we examined the mRNA expression of Pdgf ligands in CD24+ ASCs and CD24− preadipocytes in *Pdgfa* cKO mice. While *Pdgfc* was not detected (not shown) and *Pdgfd* was not altered in APs from *Pdgfa* cKO mice, *Pdgfb* was significantly upregulated in both CD24+ ASCs and CD24− preadipocytes in *Pdgfa* cKO mice at P22 when hair cycling is initiated. Given the somewhat overlapping roles of Pdgfa and Pdgfb (Chen et al., 2004; Donovan et al., 2013), Pdgfb may compensate for the lack of Pdgfa to maintain hair follicle cycling in *Pdgfa* cKO mice (Figure S3I–J).

To delineate whether Pdgfa promotes AP maintenance, we examined the number of dermal APs in *Pdgfa* cKO mice before and after hair follicle regeneration. While CD24− preadipocytes were not altered in the absence of Pdgfa signaling, CD24+ ASCs showed a 50% reduction in *Pdgfa* cKO mice at all time points examined before and after hair regrowth (Figures 3F–H). This decrease in CD24+ ASC numbers was specific to the skin as CD24+ ASCs were similar in vWAT and sWAT depots of WT and *Pdgfa* cKO mice (Figure S3K), indicating that Pdgfa signaling plays a specific role in maintaining dermal CD24+ ASCs. To determine if *Pdgfa* regulates proliferation of dermal CD24+ ASCs, we injected WT and *Pdgfa* cKO mice with EdU during hair follicle involution and at the peak of CD24+ ASC proliferation from P17 to P19 (Figure 1H). At the initiation of hair follicle cycling (P20), both CD24+ ASCs and CD24− preadipocytes displayed substantially reduced EdU incorporation in *Pdgfa* cKO mice compared to WT mice (Figure 3I–K). These data demonstrate that dermal *Pdgfa* expression is required for CD24+ ASC proliferation and maintenance in the skin.

Pdgfa acts directly on CD24+ ASCs

To determine if Pdgfa acts directly on AP cells, we performed competitive transplantation experiments to examine the maintenance of WT and *Pdgfrα* null APs in the dermis. Donor *Rosa*-CreER; mT/mG; *Pdgfrα*$^{fl/fl}$ mice were treated with tamoxifen at P21–P24 (Figure 4A) and 19% of APs were GFP+ and lacked *Pdgfrα* (Figures 4A–C). We then transplanted 2×10^5 total dTomato+ and mGFP+ AP cells into the skin of syngeneic WT hosts together, allowing us to simultaneously analyse WT and *Pdgfrα* null AP maintenance (Figure 4A). After 3 days of transplantation, the percentage of transplanted GFP+ APs recovered from the recipients was reduced to 1.8% (Figure 4D–E). Both populations of GFP+ APs, CD24+

ASC and CD24− preadipocytes, showed a significant decrease in their recovery 3 days after transplantation (Figure 4D–E). Since only 4×10^4 GFP+ APs were transplanted in these experiments, we determined if loss of transplanted APs was due to the low number of transplanted cells. Transplantation of 4×10^4 WT APs were maintained in the dermis after 10 days and formed Perilipin+, mature adipocytes (Figure S4A–B). These data suggest that lack of *Pdgfra* impacts the maintenance of APs in the skin.

Since CD24+ ASCs generate CD24− preadipocytes (Berry and Rodeheffer, 2013), we determined whether the loss of both subpopulations of APs was primarily due to a defect in CD24+ ASC proliferation. We pulsed *Rosa*-CreER; mT/mG*; Pdgfra*$^{fl/fl}$ mice with EdU for 6h at P17 or P18. While CD24-preadipocytes incorporated low amounts of EdU in both genotypes, *Pdgfra* null CD24+ ASCs incorporated significantly less EdU than WT CD24+ ASCs (Figure 4F–G). These data demonstrate that CD24+ ASCs require intrinsic Pdgf signaling for proper maintenance and proliferation.

Pdgfa signaling induces a specific gene expression signature in APs through PI3K/Akt signaling

Next, we aimed to define the molecular pathways activated by Pdgfa in dermal adipogenic cells. Since Pdgfa induced purified APs to proliferate *in vitro* (Figure S5A), we performed RNA-seq on primary dWAT APs treated with Pdgfa for 1 and 2 hr. Interestingly, the gene signature induced by Pdgfa in APs was dramatically distinct from the genes changed by Pdgfa in embryonic fibroblasts (Figure 5A) (Chen et al., 2004). Gene ontology (GO) analysis of the gene signature altered by Pdgfa treatment of APs highlighted changes in proliferation, differentiation, and survival genes (Figure 5B). Validating upregulated genes by qPCR confirmed the alterations in gene expression induced by Pdgfa in APs (Figure 5C). Pdgfa-target gene expression was also downregulated in both CD24+ ASCs and CD24− preadipocytes from P16 Pdgfa cKO mice (Figure 5D), suggesting that some of these genes are also Pdgfa-target genes *in vivo*. Ingenuity pathway analysis (IPA) indicated that activity through the phosphoinositide 3-kinase (PI3K)-Akt or the Map kinase pathways showed strong correlation with our gene expression signature (Figure S5B).

Since PI3K/Akt is activated by Pdgfa in mesenchymal cells (Fantauzzo and Soriano, 2014; Fitter et al., 2012; Liu et al., 2011), we analyzed the status of the PI3K/Akt and other pathways following Pdgfa-induced proliferation in APs. FACS-purified primary dermal APs treated with Pdgfa *in vitro* increased levels of phosphorylated Akt but not phosphorylated protein kinase C, which is primarily activated by Pdgfb (Artemenko et al., 2005; 2007) (Figure 5E). Additionally, while Pdgfa treatment induced AP proliferation *in vitro*, co-treatment of APs with Pdgfa and the PI3K/Akt inhibitor LY294002 or the Map kinase inhibitor Vemurafenib completely abrogated EdU incorporation in APs, while the Jak/Stat inhibitor Ruxolitinib had little effect. (Figure 5F–G and S5C–F). Furthermore, we found that cultured APs treated with the PI3K/Akt inhibitor LY294002 did not upregulate a subset of Pdgfa target genes when stimulated with Pdgfa (Figure 5H). These data highlight specific signaling pathways downstream of Pdgfa activation in adipogenic cells.

Given the importance of the PI3K/Akt pathway in regulating AP and mature adipocyte biology (Fischer-Posovszky et al., 2012; Jeffery et al., 2015), we analysed the activation of

Akt at serine 473 in APs *in vivo* during the hair follicle cycle using FACS. A subset of CD24+ ASCs and CD24− preadipocytes displayed activation of Akt throughout hair follicle cycling (Figure 6A and 6B). To determine whether loss of *Pdgfa* alters Akt phosphorylation in APs, we examined Akt phosphorylation in APs from *Pdgfa* cKO mice. p-Akt levels were significantly reduced in CD24+ ASCs but not CD24− preadipocytes from *Pdgfa* cKO mice (Figure 6C and 6D), indicating that Akt activity is differentially regulated in APs by Pdgfa.

The most prominent Akt family members are *Akt1* and *Akt2* (W. S. Chen et al., 2001; Cho et al., 2001a; 2001b). We previously showed that while both Akt genes are expressed by APs, *Akt2* has a prominent role in CD24+ ASC proliferation in response to high fat diet in vWAT (Jeffery et al., 2015). Yet, Pdgfa-target genes were not activated in vWAT APs in response to high fat diet, suggesting that the activation of APs during high fat diet is distinct from the Pdgfa-induced activation of CD24+ ASCs in the dermis (Figure S5G).

We next determined whether *Akt2* regulates adipogenesis in the skin. Dermal WAT formed normally in *Akt2* null mice (Figure S6A) and hair follicle regression was initiated in Akt2 KO mice with similar timing to WT mice at P16 (Figures S6A–B). We next examined whether CD24+ ASC proliferation was initiated in the absence of *Akt2* expression. Both CD24+ ASCs and CD24− preadipocytes from the skin of *Akt2* KO mice incorporated less EdU at the peak of hair follicle growth-associated CD24+ ASC proliferation (Figures 6E–G). Consistent with a defect in CD24+ ASC activity, *Akt2* KO mice displayed reduced dermal WAT in later hair growth stages (Figure 6H–I). Together, these data indicate that Pdgfa acts through Akt signaling to enhance dermal CD24+ ASC proliferation and maintain of dermal WAT.

Discussion

Although adipocyte hyperplasia occurs in several depots during obesity (Jeffery et al., 2015; Vishvanath et al., 2016) and regenerative processes in the skin (Festa et al., 2011), the cellular and molecular mechanisms that regulate adipocyte hyperplasia and maintenance are not well understood. Our previous work has established a lineage relationship whereby mature adipocytes are generated by APs in multiple depots (Berry et al., 2014; Berry and Rodeheffer, 2013; Festa et al., 2011; Jeffery et al., 2015). Here, we show that a subpopulation of APs, CD24+ ASCs, are diminished with age and activated during hair follicle associated dWAT regression and prior to hair follicle stem cell activation, which is consistent with the ability of APs to induce hair cycling (Festa et al., 2011). It is interesting to speculate that signals from atrophied intradermal adipocytes may stimulate activation of CD24+ ASCs during the hair cycle, which has been hypothesized during obesity in other WAT depots (Jeffery et al., 2015; Lee et al., 2013). AP differentiation is also activated by signals from the growing hair follicle (Donati et al., 2014). Given the expansion of dWAT during hair cycling (Festa et al., 2011), cold stress (Alexander et al., 2015), and bacterial infection (Zhang et al., 2015), Pdgfa-initiated intradermal adipocyte hyperplasia may occur in several physiological contexts.

A functional picture of mesenchymal heterogeneity in the skin is emerging in the field. While several stem cell populations exist within epidermal keratinocyte compartments in the

epidermis and pilosebaceous unit (Goldstein and Horsley, 2012), less is understood about the maintenance of mesenchymal heterogeneity within the dermis. Recent work highlighted the developmental origins of mesenchymal fibroblasts and showed that precursors for dWAT and the upper dermal fibroblasts become distinct during development (Driskell et al., 2013). Specialized dermal fibroblasts called dermal papillae provide instructive, growth and regenerative signals for the hair follicle (Chi et al., 2013; Clavel et al., 2012; Jahoda et al., 1984; Rompolas et al., 2012) and may be maintained by fibroblasts in the dermal sheath cell surrounding the hair follicle (Rahmani et al., 2014). Our data provide further evidence for mesenchymal heterogeneity within the dermis by elucidating mechanisms that maintain CD24+ ASCs.

Our data reveal distinct mechanisms that regulate hyperplasia in individual WAT depots. Hyperplasia of WAT during obesity occurs with different timescales in different depots (Berry and Rodeheffer, 2013; Birsoy et al., 2011; Han et al., 2011; Wang et al., 2013). We recently showed that during high fat diet feeding of male mice, CD24+ ASCs are activated to proliferate and induce vWAT hyperplasia but that CD24+ ASCs in sWAT remain quiescent (Jeffery et al., 2016; 2015). Here, we identify a mechanism that regulates CD24+ ASC activation specifically in dWAT, further supporting that individual WAT depots provide a unique microenvironment to regulate CD24+ ASC activation and adipogenesis. This theme is similar to the heterogeneity of muscle stem cell activity within individual skeletal muscles (Yin et al., 2013).

dWAT CD24+ ASC self-renewal and proliferation partially relies on Pdgfa/Pdgfrα-signaling and is consistent with the loss of dWAT in constitutive Pdgfa deletion in mice (Karlsson et al., 1999). While Pdgfb/Pdgfrβ signaling can abrogate adipocyte differentiation *in vivo* (Olson and Soriano, 2011) and *in vitro* (Artemenko et al., 2005; Fitter et al., 2012), the endogenous role of Pdgfa in adipogenesis *in vivo* is less well understood. Interestingly, constitutive activation of Pdgfrα in Pdgfrα-expressing cells or in a subset of *Nestin*-expressing dermal cells leads to loss of dWAT and skin fibrosis phenotypes, which may be in part related to the ability of Pdgf signaling to inhibit adipogenic differentiation (Iwayama et al., 2015; Olson and Soriano, 2009). Our data resonate with the ability of Pdgfa to control glioblastoma cancer stem cell self-renewal (Gong et al., 2015) and Pdgfrα activation in pancreatic β-cell expansion and age-dependent proliferation (H. Chen et al., 2011).

While Pdgfa signaling can act through multiple pathways, several studies have indicated that Pdgfa signals through the PI3K cascade in mesenchymal cells (Fantauzzo and Soriano, 2014; Iwayama et al., 2015; Rosenkranz et al., 1999). Our data suggests that PI3K/Akt plays a major role in transducing Pdgfa signaling in CD24+ ASCs. We recently identified that obesogenic stimuli activate PI3K/Akt2 signaling to induce for CD24+ ASC proliferation and vWAT hyperplasia (Jeffery et al., 2015) and Akt2 has also been shown to act at later stages of adipogenesis including lipogenesis (Leavens et al., 2009). Thus, WAT depot specific mechanisms that activate PI3K/Akt2 signaling are involved in multiple modes of adipogenic regulation. Future studies dissecting the direct targets of Akt2 in APs may reveal novel regulatory genes involved in WAT hyperplasia in multiple depots.

In summary, we provide evidence that CD24+ adipocyte stem cells harbor self-renewal and proliferative capacity that is essential for dWAT maintenance. Our data clarify the function of Pdgfa in dermal mesenchymal cells and shed light on the regulation of CD24+ ASCs *in vivo*. Given the importance of dWAT expansion in infection, hair growth, wound healing and thermal regulation, our findings have implications toward understanding pathological mechanisms by which adipogenesis defects may contribute to skin disorders. Finally, since adipocytes exist within depots associated with the mammary gland and skeletal muscle, our results may shed light on how adipocytes in other adipose depots are regulated.

Experimental procedures

Mice and chemical treatments

All experiments conducted on mice were done following the guidelines issued by Yale's University Institutional Animal Care and Use Committee (IACUC). C57/Bl6 mice were purchased from Charles River Laboratories and used at least one week after their arrival. Pdgfrα-Cre (*C57BL/6-tg(PdgfRa-cre01Clc/J*, stock #013148), mT/mG (*B6.129(Cg)–Gt(ROSA)26Sortm4(ACTB–tdTomato,– EGFP)Luo/J*, stock # 007676; *Pdgfra*^{fl} (*B6.Cg-Pdgfratm8Sor/EiJ*, stock # 006492); *Rosa*-CreER (*B6.129-Gt(ROSA)26Sortm1(cre/ERT2)Tyj/J*, stock # 008463) were purchased from Jackson Laboratories. *Adiponectin-CreER* mice were provided by E. Rosen (Beth Israel Deaconess Medical Center, Boston, MA, USA) and are now available at Jackson Laboratories (stock #024671). *Pdgfa*^{fl} mice were a generous gift from Christer Betsholtz (Uppsala University, Sweden). Aged mice (18, 24 and 30 month old) were obtained from the NIA. *Akt2* KO mice were a generous gift from W. Sessa (Yale University, New Haven, CT, USA). A 30mg/ml tamoxifen stock (Sigma T5648) was generated in 100μl of ethanol (200 proof; Decon Laboratories #2716) and 900μl sesame oil (Sigma S3547) and administered at 100mg/kg/day via intraperitoneal injection. For *in vivo* proliferation assays mice were injected with 5-ethynyl-2′-deoxyuridine (EdU) (Invitrogen A10044) by intraperitoneal injection using a 50mg/kg of weight dose.

Immunofluorescence and tissue staining

Mouse skin was embedded in OCT compound (Tissue-Trek 4583) and frozen on dry ice. OCT blocks were cryosectioned at 14μm and fixed for 10 min with 4% formaldehyde. Skin sections were stained as previously described (Festa et al., 2011). The following antibodies were used: GFP (chicken, Abcam (ab13970), 1:1000), Perilipin A (goat, Abcam (ab61682), 1:1000). Sections were mounted in Prolong Gold anti-fade reagent with 4′6′-diamidino-2-phenylindole (DAPI) (Invitrogen P36935). For skin whole mount staining, skin strips (approximately 1 mm thick) were obtained and fixed in 4% paraformaldehyde for 20 min. Skin strips were then washed with PBS and stained with Bodipy (1:1000, Invitrogen D-3922) and TO-PRO-3 Iodide (1:300, Thermo Fisher Scientific T3605) for 30 min at room temperature. Strips were washed in PBS and mounted using Aqua Poly/Mount (Polysciences 18606). Images were acquired in a LSM 510 Visible Confocal microscope (Zeiss) using the ZEN software. Image analysis and measurements were done using ImageJ software (NIH) and Adobe Photoshop.

Flow activated cell sorting and analysis

FACS analysis of APs was performed as described previously (Festa et al., 2011; Jeffery et al., 2015). Briefly, mouse skin was dissected and digested in collagenase buffer (HBSS containing 3% BSA, Collagenase 1A 1:100, Worthington LS004196, 1.2mM calcium chloride, 0.8mM zinc chloride) for 60 min at 37°C in a shaking water bath. Undigested tissue was separated from released cells through filtration using 70μm filters. Floating mature adipocytes were separated from the stromal vascular fraction (SVF) by centrifugation at 300g for 3 min. To identify adipocyte precursors (APs) SVF was stained in 3% BSA in HBSS with the following antibodies: CD31-PE-Cy7 (1:500, eBioscience 25-0311-82), CD45 APC-eFluor 780 (1:5000, eBioscience 47-0451-82) CD29 Alexa Fluor 700 (1:400, Biolegend 102218), CD34 Brilliant Violet 421 (1:50, Biolegend 119321) Ly-6A/E (Sca1) V500 (1:500, BD Biosciences, 561229) and CD24 PerCP-Cy5.5 (1:200, eBioscience 45-0242-82). For live/dead discrimination, cells were stained with Sytox Orange (1:100,000, Invitrogen S11368). For analysis of proliferation by EdU incorporation, the Click-iT EdU Flow Cytometry Assay Kit (Invitrogen C10419) was used following the manufacturer's instructions. Detection of phosphorylated Akt in APs was performed as previously described (Jeffery et al., 2015) using pAkt S473 (1:50; Cell Signaling 9271). Samples were sorted or analyzed with a FACS Aria III with DiVA software. Analysis of flow cytometry data was performed using FlowJo Software.

Adipocyte precursor cell culture

FACS-isolated APs were cultured as described (Festa et al., 2011; Rodeheffer et al., 2008). FACS sorted cells were plated on carboxyl-coated 24 well plates (BD Biosciences 354775) in DMEM supplemented with 10% FBS. AT 50% confluency, APs were switched to 0.5% FBS DMEM overnight and treated with Pdgfa (30ng/ml, Affimetryx/eBioscience 14-8989-80) or vehicle 1% BSA in PBS for specific periods of time. For proliferation assays APs were treated with Pdgfa (30ng/ml, Affimetryx/eBioscience 14-8989-80), 5μM EdU, LY294002 (2μM, Selleckchem S1105), Vemurafenib (1μM, Selleckchem, S1267) and Ruxolitinib (5μM, Selleckchem, S1378) or DMSO for 24h.

RNA extraction and Real-Time PCR

APs were either sorted directly into Trizol LS (Invitrogen 10296-028) or lysed in 24 well plates by adding Trizol (Invitrogen 15596-026). RNA extraction and purification was done using the RNeasy mini kit (QIAGEN 74104) following manufacturer instructions. cDNA was generated using equal amounts of total RNA with the Superscript III First-Strand Synthesis System (Invitrogen 18080051) using Oligo dT per the manufacturer's instructions. Real time PCR was performed as previously described (Festa et al., 2011) using SYBR green I Master mix (Roche 04887352001) on a LightCycler 480 (Roche). Primers for specific genes are listed in the supplemental information section. Results were normalized to β-actin expression as described previously (Festa et al., 2011).

Western Blot

Adipocyte precursors were processed as previously described (Goldstein et al., 2014). Briefly, APs were collected in RIPA buffer supplemented with protease inhibitors. Equal

amount of protein lysates were loaded into acrylamide SDS-PAGE gels, blotted into PVDF membranes and developed by chemiluminescence. The following primary antibodies were used: Akt (1:500, Cell Signaling 9272), pAkt Ser473 (1:500, Cell Signaling 9271), PKC (1:500, Abcam ab19031), pPKC βII Ser660 (1:500 Cell Signaling 9371) and β-actin (1:3000, Sigma AC-15).

Competitive transplantation assay

APs cells were isolated by FACS from *Rosa-CreER; mT/mG; Pdgfra*$^{fl/fl}$ injected with tamoxifen for four days as described above. Isolated APs included WT (Tomato+) and Pdgfrα KO (GFP+) that were injected intradermally into the back skin of P14 *Rosa-CreER; Pdgfra*$^{fl/fl}$ male mice. Each recipient mouse was injected with 200,000 APs, at two different sites, one closer to the anterior and another closer to the posterior area. At P17 the skin of recipient mice was analysed for the presence of both WT (Tomato+) and *Pdgfra* KO (GFP+) APs using the FACS strategy described previously.

RNA-seq

RNA samples were prepared from primary APs isolated from the back skin of four 6 week old C57/Bl6 mice and treated with Pdgfa for 1 or 2 hours or left untreated as described above. RNA from the different samples was pooled and RNA-seq was performed as described previously (Tadeu et al., 2015). Single-end RNA sequencing was done using an Illumina sequencer at the Yale Center for Genome Analysis. Using the TopHat and Cufflinks suite (Roberts et al., 2012), the raw reads were assembled into a transcriptome, and a list of differentially expressed and regulated genes and transcripts was produced. Gene Ontology analysis was done on the significantly regulated genes (experimental logarithmic ratio < 1, $p < 0.05$ and $q < 0.05$) using DAVID (Huang et al., 2009a; 2009b) or the QIAGEN's Ingenuity® Pathway Analysis software suite (IPA®, QIAGEN Redwood City, www.qiagen.com/ingenuity). RNA-seq data was deposited to the GEO database accession number GSE84370.

Statistics

To determine statistical significance between more than two groups a one-way ANOVA was used. Comparisons between two groups were made using Student's t-test using GraphPad Prism for Mac (GraphPad Software). Statistical significance was set at $p<0.05$.

Supplementary Material

Refer to Web version on PubMed Central for supplementary material.

Acknowledgments

We thank Horsley and Rodeheffer lab members for technical assistance, critical reading of the manuscript and scientific discussions. We thank Kaitlyn M. Sabin for technical assistance with section staining and imaging. This project was funded by the NIA through the pilot project grants from the Claude D. Pepper Older Americans Independence Center at Yale (NIA P30AG21342) awarded to V.H. and (NIA P30AG21342) awarded to M.S.R. This work was also supported by grants from NIDDK (R01DK090489) to M.S.R and NIAMS (AR060296) awarded to V.H.

References

Adam RC, Yang H, Rockowitz S, Larsen SB, Nikolova M, Oristian DS, Polak L, Kadaja M, Asare A, Zheng D, Fuchs E. Pioneer factors govern super-enhancer dynamics in stem cell plasticity and lineage choice. Nature. 2015; 521:366–370. DOI: 10.1038/nature14289 [PubMed: 25799994]

Alexander CM, Kasza I, Yen C-LE, Reeder SB, Hernando D, Gallo RL, Jahoda CAB, Horsley V, MacDougald OA. Dermal white adipose tissue: a new component of the thermogenic response. J Lipid Res. 2015; 56:2061–2069. DOI: 10.1194/jlr.R062893 [PubMed: 26405076]

Andrae J, Gouveia L, He L, Betsholtz C. Characterization of platelet-derived growth factor-A expression in mouse tissues using a lacZ knock-in approach. PLoS ONE. 2014; 9:e105477.doi: 10.1371/journal.pone.0105477 [PubMed: 25166724]

Arner P, Andersson DP, Thörne A, Wirén M, Hoffstedt J, Näslund E, Thorell A, Rydén M. Variations in the size of the major omentum are primarily determined by fat cell number. J Clin Endocrinol Metab. 2013; 98:E897–901. DOI: 10.1210/jc.2012-4106 [PubMed: 23543656]

Artemenko Y, Gagnon A, Aubin D, Sorisky A. Anti-adipogenic effect of PDGF is reversed by PKC inhibition. J Cell Physiol. 2005; 204:646–653. DOI: 10.1002/jcp.20314 [PubMed: 15754337]

Artemenko Y, Gagnon A, Ibrahim S, Sorisky A. Regulation of PDGF-stimulated SHIP2 tyrosine phosphorylation and association with Shc in 3T3-L1 preadipocytes. J Cell Physiol. 2007; 211:598–607. DOI: 10.1002/jcp.20965 [PubMed: 17219406]

Beerman I, Rossi DJ. Epigenetic Control of Stem Cell Potential during Homeostasis, Aging, and Disease. Cell Stem Cell. 2015; 16:613–625. DOI: 10.1016/j.stem.2015.05.009 [PubMed: 26046761]

Berry R, Jeffery E, Rodeheffer MS. Weighing in on adipocyte precursors. Cell Metabolism. 2014; 19:8–20. DOI: 10.1016/j.cmet.2013.10.003 [PubMed: 24239569]

Berry R, Rodeheffer MS. Characterization of the adipocyte cellular lineage in vivo. Nat Cell Biol. 2013; 15:302–308. DOI: 10.1038/ncb2696 [PubMed: 23434825]

Birsoy K, Berry R, Wang T, Ceyhan O, Tavazoie S, Friedman JM, Rodeheffer MS. Analysis of gene networks in white adipose tissue development reveals a role for ETS2 in adipogenesis. Development. 2011; 138:4709–4719. DOI: 10.1242/dev.067710 [PubMed: 21989915]

Chase HB, Montagna W, MALONE JD. Changes in the skin in relation to the hair growth cycle. Anat Rec. 1953; 116:75–81. [PubMed: 13050993]

Chen H, Gu X, Liu Y, Wang J, Wirt SE, Bottino R, Schorle H, Sage J, Kim SK. PDGF signalling controls age-dependent proliferation in pancreatic β-cells. Nature. 2011; 478:349–355. DOI: 10.1038/nature10502 [PubMed: 21993628]

Chen WS, Xu PZ, Gottlob K, Chen ML, Sokol K, Shiyanova T, Roninson I, Weng W, Suzuki R, Tobe K, Kadowaki T, Hay N. Growth retardation and increased apoptosis in mice with homozygous disruption of the Akt1 gene. Genes & Development. 2001; 15:2203–2208. DOI: 10.1101/gad.913901 [PubMed: 11544177]

Chen WV, Delrow J, Corrin PD, Frazier JP, Soriano P. Identification and validation of PDGF transcriptional targets by microarray-coupled gene-trap mutagenesis. Nat Genet. 2004; 36:304–312. DOI: 10.1038/ng1306 [PubMed: 14981515]

Chi W, Wu E, Morgan BA. Dermal papilla cell number specifies hair size, shape and cycling and its reduction causes follicular decline. Development. 2013; 140:1676–1683. DOI: 10.1242/dev.090662 [PubMed: 23487317]

Cho H, Mu J, Kim JK, Thorvaldsen JL, Chu Q, Crenshaw EB, Kaestner KH, Bartolomei MS, Shulman GI, Birnbaum MJ. Insulin resistance and a diabetes mellitus-like syndrome in mice lacking the protein kinase Akt2 (PKB beta). Science. 2001a; 292:1728–1731. DOI: 10.1126/science.292.5522.1728 [PubMed: 11387480]

Cho H, Thorvaldsen JL, Chu Q, Feng F, Birnbaum MJ. Akt1/PKBalpha is required for normal growth but dispensable for maintenance of glucose homeostasis in mice. J Biol Chem. 2001b; 276:38349–38352. DOI: 10.1074/jbc.C100462200 [PubMed: 11533044]

Clavel C, Grisanti L, Zemla R, Rezza A, Barros R, Sennett R, Mazloom AR, Chung CY, Cai X, Cai CL, Pevny L, Nicolis S, Ma'ayan A, Rendl M. Sox2 in the dermal papilla niche controls hair growth by fine-tuning BMP signaling in differentiating hair shaft progenitors. Dev Cell. 2012; 23:981–994. DOI: 10.1016/j.devcel.2012.10.013 [PubMed: 23153495]

Cleary MP, Brasel JA, Greenwood MR. Developmental changes in thymidine kinase, DNA, and fat cellularity in Zucker rats. Am J Physiol. 1979; 236:E508–13. [PubMed: 443370]

Cristancho AG, Lazar MA. Forming functional fat: a growing understanding of adipocyte differentiation. Nat Rev Mol Cell Biol. 2011; 12:722–734. DOI: 10.1038/nrm3198 [PubMed: 21952300]

Donati G, Proserpio V, Lichtenberger BM, Natsuga K, Sinclair R, Fujiwara H, Watt FM. Epidermal Wnt/β-catenin signaling regulates adipocyte differentiation via secretion of adipogenic factors. Proceedings of the National Academy of Sciences. 2014; 111:E1501–9. DOI: 10.1073/pnas.1312880111

Donati G, Watt FM. Stem cell heterogeneity and plasticity in epithelia. Cell Stem Cell. 2015; 16:465–476. DOI: 10.1016/j.stem.2015.04.014 [PubMed: 25957902]

Donovan J, Shiwen X, Norman J, Abraham D. Platelet-derived growth factor alpha and beta receptors have overlapping functional activities towards fibroblasts. Fibrogenesis Tissue Repair. 2013; 6:10.doi: 10.1186/1755-1536-6-10 [PubMed: 23663505]

Driskell RR, Lichtenberger BM, Hoste E, Kretzschmar K, Simons BD, Charalambous M, Ferron SR, Herault Y, Pavlovic G, Ferguson-Smith AC, Watt FM. Distinct fibroblast lineages determine dermal architecture in skin development and repair. Nature. 2013; 504:277–281. DOI: 10.1038/nature12783 [PubMed: 24336287]

Fantauzzo KA, Soriano P. PI3K-mediated PDGFR signaling regulates survival and proliferation in skeletal development through p53-dependent intracellular pathways. Genes & Development. 2014; 28:1005–1017. DOI: 10.1101/gad.238709.114 [PubMed: 24788519]

Faust IM, Johnson PR, Stern JS, Hirsch J. Diet-induced adipocyte number increase in adult rats: a new model of obesity. Am J Physiol. 1978; 235:E279–86. [PubMed: 696822]

Festa E, Fretz J, Berry R, Schmidt B, Rodeheffer M, Horowitz M, Horsley V. Adipocyte Lineage Cells Contribute to the Skin Stem Cell Niche to Drive Hair Cycling. Cell. 2011; 146:761–771. DOI: 10.1016/j.cell.2011.07.019 [PubMed: 21884937]

Fischer-Posovszky P, Tews D, Horenburg S, Debatin KM, Wabitsch M. Differential function of Akt1 and Akt2 in human adipocytes. Molecular and Cellular Endocrinology. 2012; 358:135–143. DOI: 10.1016/j.mce.2012.03.018 [PubMed: 22480544]

Fitter S, Vandyke K, Gronthos S, Zannettino ACW. Suppression of PDGF-induced PI3 kinase activity by imatinib promotes adipogenesis and adiponectin secretion. J Mol Endocrinol. 2012; 48:229–240. DOI: 10.1530/JME-12-0003 [PubMed: 22474082]

Freytag SO. Enforced expression of the c-myc oncogene inhibits cell differentiation by precluding entry into a distinct predifferentiation state in G0/G1. Mol Cell Biol. 1988; 8:1614–1624. [PubMed: 2454393]

Goldstein J, Fletcher S, Roth E, Wu C, Chun A, Horsley V. Calcineurin/Nfatc1 signaling links skin stem cell quiescence to hormonal signaling during pregnancy and lactation. Genes & Development. 2014; 28:983–994. DOI: 10.1101/gad.236554.113 [PubMed: 24732379]

Goldstein J, Horsley V. Home sweet home: skin stem cell niches. Cell Mol Life Sci. 2012; doi: 10.1007/s00018-012-0943-3

Gong A-H, Wei P, Zhang S, Yao J, Yuan Y, Zhou A-D, Lang FF, Heimberger AB, Rao G, Huang S. FoxM1 Drives a Feed-Forward STAT3-Activation Signaling Loop That Promotes the Self-Renewal and Tumorigenicity of Glioblastoma Stem-like Cells. Cancer Res. 2015; 75:2337–2348. DOI: 10.1158/0008-5472.CAN-14-2800 [PubMed: 25832656]

Goodell MA, Nguyen H, Shroyer N. Somatic stem cell heterogeneity: diversity in the blood, skin and intestinal stem cell compartments. Nat Rev Mol Cell Biol. 2015; 16:299–309. DOI: 10.1038/nrm3980 [PubMed: 25907613]

Han J, Lee JE, Jin J, Lim JS, Oh N, Kim K, Chang SI, Shibuya M, Kim H, Koh GY. The spatiotemporal development of adipose tissue. Development. 2011; 138:5027–5037. DOI: 10.1242/dev.067686 [PubMed: 22028034]

Hansen LS, Coggle JE, Wells J, Charles MW. The influence of the hair cycle on the thickness of mouse skin. Anat Rec. 1984; 210:569–573. DOI: 10.1002/ar.1092100404 [PubMed: 6524697]

Huang DW, Sherman BT, Lempicki RA. Bioinformatics enrichment tools: paths toward the comprehensive functional analysis of large gene lists. Nucleic Acids Research. 2009a; 37:1–13. DOI: 10.1093/nar/gkn923 [PubMed: 19033363]

Huang DW, Sherman BT, Lempicki RA. Systematic and integrative analysis of large gene lists using DAVID bioinformatics resources. Nature Protocols. 2009b; 4:44–57. DOI: 10.1038/nprot.2008.211 [PubMed: 19131956]

Iwayama T, Steele C, Yao L, Dozmorov MG, Karamichos D, Wren JD, Olson LE. PDGFRα signaling drives adipose tissue fibrosis by targeting progenitor cell plasticity. Genes & Development. 2015; doi: 10.1101/gad.260554.115

Jahoda CA, Horne KA, Oliver RF. Induction of hair growth by implantation of cultured dermal papilla cells. Nature. 1984; 311:560–562. [PubMed: 6482967]

Jeffery E, Berry R, Church CD, Yu S, Shook BA, Horsley V, Rosen ED, Rodeheffer MS. Characterization of Cre recombinase models for the study of adipose tissue. Adipocyte. 2014; 3:206–211. DOI: 10.4161/adip.29674 [PubMed: 25068087]

Jeffery E, Church CD, Holtrup B, Colman L, Rodeheffer MS. Rapid depot-specific activation of adipocyte precursor cells at the onset of obesity. Nat Cell Biol. 2015; 17:376–385. DOI: 10.1038/ncb3122 [PubMed: 25730471]

Jeffery E, Wing A, Holtrup B, Sebo Z, Kaplan JL, Saavedra-Peña R, Church CD, Colman L, Berry R, Rodeheffer MS. The Adipose Tissue Microenvironment Regulates Depot-Specific Adipogenesis in Obesity. Cell Metabolism. 2016; doi: 10.1016/j.cmet.2016.05.012

Karlsson LL, Bondjers CC, Betsholtz CC. Roles for PDGF-A and sonic hedgehog in development of mesenchymal components of the hair follicle. Development. 1999; 126:2611–2621. [PubMed: 10331973]

Kasza I, Suh Y, Wollny D, Clark RJ, Roopra A, Colman RJ, MacDougald OA, Shedd TA, Nelson DW, Yen M-I, Yen C-LE, Alexander CM. Syndecan-1 is required to maintain intradermal fat and prevent cold stress. PLoS Genet. 2014; 10:e1004514.doi: 10.1371/journal.pgen.1004514 [PubMed: 25101993]

Keyes BE, Segal JP, Heller E, Lien WH, Chang CY, Guo X, Oristian DS, Zheng D, Fuchs E. Nfatc1 orchestrates aging in hair follicle stem cells. Proceedings of the National Academy of Sciences. 2013; 110:E4950–9. DOI: 10.1073/pnas.1320301110

Leavens KF, Easton RM, Shulman GI, Previs SF, Birnbaum MJ. Akt2 is required for hepatic lipid accumulation in models of insulin resistance. Cell Metabolism. 2009; 10:405–418. DOI: 10.1016/j.cmet.2009.10.004 [PubMed: 19883618]

Lee YH, Petkova AP, Granneman JG. Identification of an adipogenic niche for adipose tissue remodeling and restoration. Cell Metabolism. 2013; 18:355–367. DOI: 10.1016/j.cmet.2013.08.003 [PubMed: 24011071]

Lemonnier D. Effect of age, sex, and sites on the cellularity of the adipose tissue in mice and rats rendered obese by a high-fat diet. J Clin Invest. 1972; 51:2907–2915. DOI: 10.1172/JCI107115 [PubMed: 5080416]

Liu S, Liu S, Wang X, Zhou J, Cao Y, Wang F, Duan E. The PI3K-Akt pathway inhibits senescence and promotes self-renewal of human skin-derived precursors in vitro. Aging Cell. 2011; 10:661–674. DOI: 10.1111/j.1474-9726.2011.00704.x [PubMed: 21418510]

Luo Y, Toyoda M, Nakamura M, Morohashi M. Morphological analysis of skin in senescence-accelerated mouse P10. Med Electron Microsc. 2002; 35:31–45. DOI: 10.1007/s007950200004 [PubMed: 12111405]

Muzumdar MD, Tasic B, Miyamichi K, Li L, Luo L. A global double-fluorescent Cre reporter mouse. Genesis. 2007; 45:593–605. DOI: 10.1002/dvg.20335 [PubMed: 17868096]

Olson LE, Soriano P. PDGFRβ signaling regulates mural cell plasticity and inhibits fat development. Dev Cell. 2011; 20:815–826. DOI: 10.1016/j.devcel.2011.04.019 [PubMed: 21664579]

Olson LE, Soriano P. Increased PDGFRalpha activation disrupts connective tissue development and drives systemic fibrosis. Dev Cell. 2009; 16:303–313. DOI: 10.1016/j.devcel.2008.12.003 [PubMed: 19217431]

Pellettieri J, Sánchez Alvarado A. Cell turnover and adult tissue homeostasis: from humans to planarians. Annu Rev Genet. 2007; 41:83–105. DOI: 10.1146/annurev.genet.41.110306.130244 [PubMed: 18076325]

Rahmani W, Abbasi S, Hagner A, Raharjo E, Kumar R, Hotta A, Magness S, Metzger D, Biernaskie J. Hair follicle dermal stem cells regenerate the dermal sheath, repopulate the dermal papilla, and modulate hair type. Dev Cell. 2014; 31:543–558. DOI: 10.1016/j.devcel.2014.10.022 [PubMed: 25465495]

Roberts A, Goff L, Pertea G, Kim D, Kelley DR, Pimentel H, Salzberg SL, Rinn JL, Pachter L, Trapnell C. Differential gene and transcript expression analysis of RNA-seq experiments with TopHat and Cufflinks. Nature Protocols. 2012; 7:562–578. DOI: 10.1038/nprot.2012.016 [PubMed: 22383036]

Rodeheffer MS, Birsoy K, Friedman JM. Identification of White Adipocyte Progenitor Cells In Vivo. Cell. 2008; 135:240–249. DOI: 10.1016/j.cell.2008.09.036 [PubMed: 18835024]

Rompolas P, Deschene ER, Zito G, Gonzalez DG, Saotome I, Haberman AM, Greco V. Live imaging of stem cell and progeny behaviour in physiological hair-follicle regeneration. Nature –. 2012; doi: 10.1038/nature11218

Rosenkranz S, DeMali KA, Gelderloos JA, Bazenet C, Kazlauskas A. Identification of the receptor-associated signaling enzymes that are required for platelet-derived growth factor-AA-dependent chemotaxis and DNA synthesis. J Biol Chem. 1999; 274:28335–28343. [PubMed: 10497192]

Shugart EC, Umek RM. Dexamethasone signaling is required to establish the postmitotic state of adipocyte development. Cell Growth Differ. 1997; 8:1091–1098. [PubMed: 9342187]

Spalding KL, Arner E, Westermark PO, Bernard S, Buchholz BA, Bergmann O, Blomqvist L, Hoffstedt J, Näslund E, Britton T, Concha H, Hassan M, Rydén M, Frisén J, Arner P. Dynamics of fat cell turnover in humans. Nature. 2008; 453:783–787. DOI: 10.1038/nature06902 [PubMed: 18454136]

Sun LQ, Lee DW, Zhang Q, Xiao W, Raabe EH, Meeker A, Miao D, Huso DL, Arceci RJ. Growth retardation and premature aging phenotypes in mice with disruption of the SNF2-like gene, PASG. Genes & Development. 2004; 18:1035–1046. DOI: 10.1101/gad.1176104 [PubMed: 15105378]

Tadeu AMB, Lin S, Hou L, Chung L, Zhong M, Zhao H, Horsley V. Transcriptional profiling of ectoderm specification to keratinocyte fate in human embryonic stem cells. PLoS ONE. 2015; 10:e0122493.doi: 10.1371/journal.pone.0122493 [PubMed: 25849374]

Tchkonia T, Morbeck DE, Von Zglinicki T, Van Deursen J, Lustgarten J, Scrable H, Khosla S, Jensen MD, Kirkland JL. Fat tissue, aging, and cellular senescence. Aging Cell. 2010; 9:667–684. DOI: 10.1111/j.1474-9726.2010.00608.x [PubMed: 20701600]

Tyner SD, Venkatachalam S, Choi J, Jones S, Ghebranious N, Igelmann H, Lu X, Soron G, Cooper B, Brayton C, Park SH, Thompson T, Karsenty G, Bradley A, Donehower LA. p53 mutant mice that display early ageing-associated phenotypes. Nature. 2002; 415:45–53. DOI: 10.1038/415045a [PubMed: 11780111]

Vishvanath L, MacPherson KA, Hepler C, Wang QA, Shao M, Spurgin SB, Wang MY, Kusminski CM, Morley TS, Gupta RK. Pdgfrβ (+) Mural Preadipocytes Contribute to Adipocyte Hyperplasia Induced by High-Fat-Diet Feeding and Prolonged Cold Exposure in Adult Mice. Cell Metabolism. 2016; 23:350–359. DOI: 10.1016/j.cmet.2015.10.018 [PubMed: 26626462]

Wang QA, Tao C, Gupta RK, Scherer PE. Tracking adipogenesis during white adipose tissue development, expansion and regeneration. Nature Medicine. 2013; doi: 10.1038/nm.3324

Yin H, Price F, Rudnicki MA. Satellite cells and the muscle stem cell niche. Physiol Rev. 2013; 93:23–67. DOI: 10.1152/physrev.00043.2011 [PubMed: 23303905]

Zhang LJ, Guerrero-Juarez CF, Hata T, Bapat SP, Ramos R, Plikus MV, Gallo RL. Innate immunity. Dermal adipocytes protect against invasive Staphylococcus aureus skin infection. Science. 2015; 347:67–71. DOI: 10.1126/science.1260972 [PubMed: 25554785]

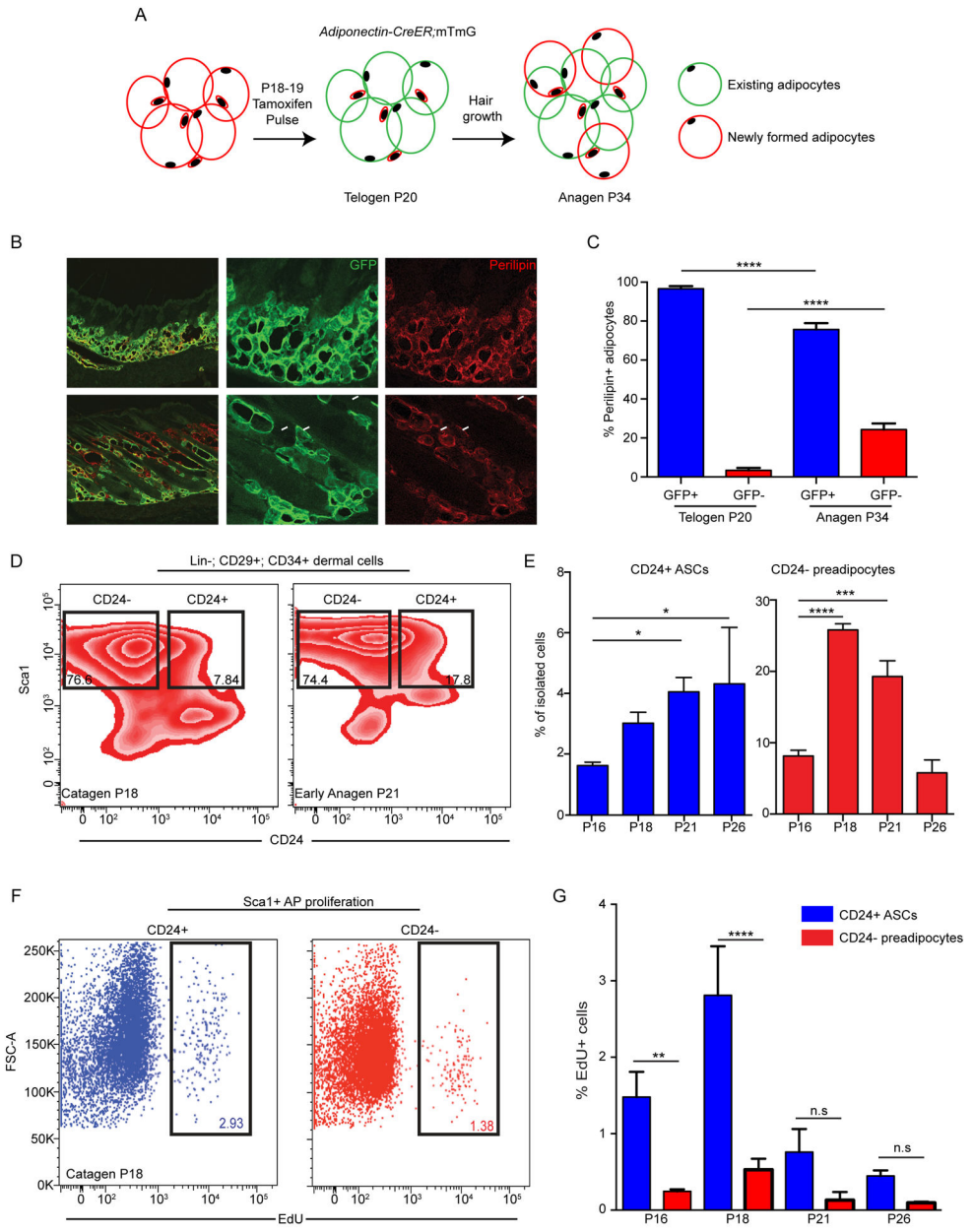

Figure 1. Adipogenesis in the skin and activation of AP cells during the telogen-anagen transition

A. Experimental scheme for analysis of *in vivo* adipogenesis with the *Adiponectin*-CreER;mTmG mouse model. **B–C**. Representative images (B) and quantification (C) of adipocyte tracing in *Adiponectin*-CreER;mTmG mice after tamoxifen treatment at P18–19 and analysis at P20 (Telogen) or at P34 (Anagen). Sections were stained for with GFP and perilipin1A antibodies. Scale bar is 200μm. (n = 4 mice for each time point). **D–E**. Flow cytometry plots (D) and quantification (E) of Lin-: CD29+:CD34+:Sca1+ gated on CD24+ adipocyte stem cell (ASC) or CD24− preadipocytes throughout hair regeneration. The percentage of AP cells is shown in each gate (D). (n = 3–4 mice for each time point). **F–G**. Flow cytometry analysis (F) and quantification (G) of EdU-positive CD24+ and CD24− intradermal APs. Mice were injected with EdU 6h prior to each time point. (n = 3–4 mice).

Data are mean ± SD. Asterisk indicates significance, *p<0.05, **p<0.01, ***p< 0.001 or **** p<0.0001 calculated with One-way ANOVA with Dunett's or Tukey's post-test for multiple comparisons. See also Figure S1.

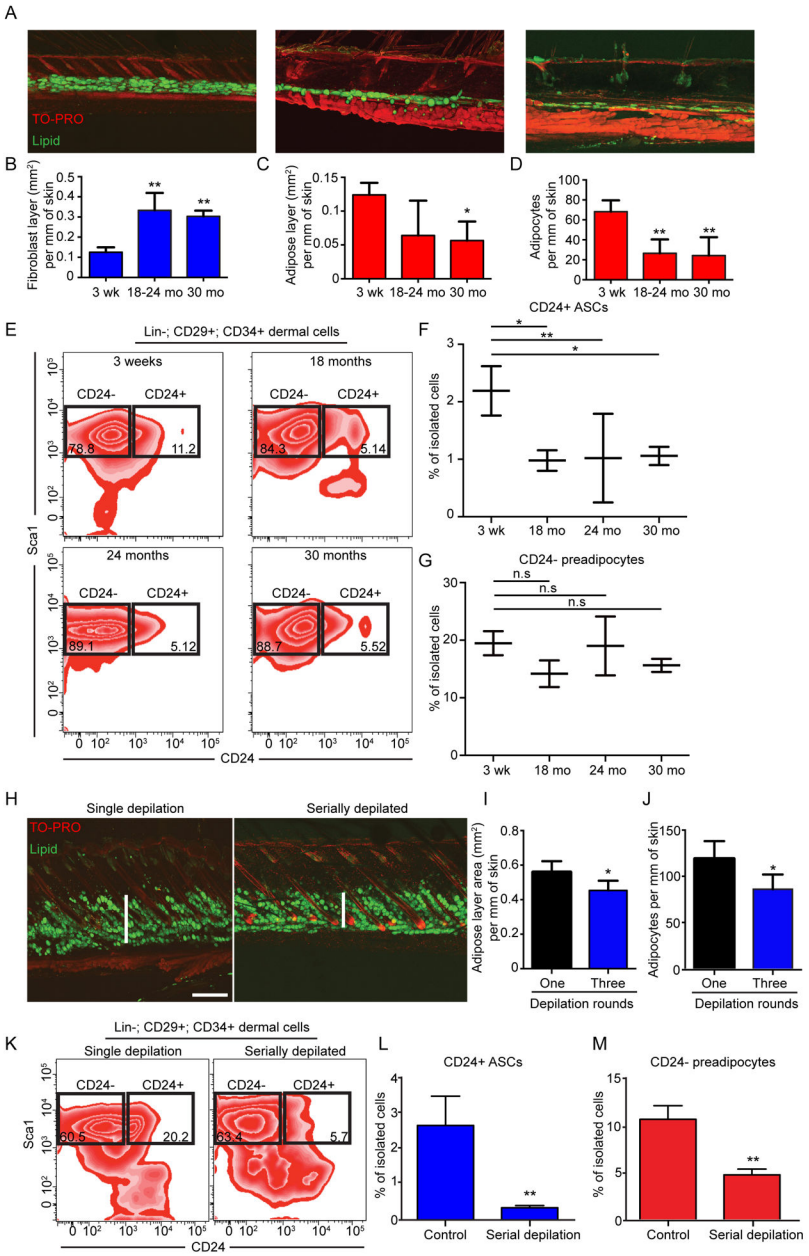

Figure 2. Loss of adipose tissue in different models correlates with loss of APs

A. Whole mounts images of C57/Bl6 skin stained with stained with bodipy to label neutral lipids and TOPRO-3 at different indicated ages. Scale bar is 200μm**. B–D.** Quantification of the area of the fibroblast-rich dermis (B) or the dermal adipose layer (C) and the number of mature adipocytes (D) normalized to skin length. (*n* = 3–5 mice for each time point). **E–F**. FACS plots and quantification of dermal CD24+ adipocyte stem cells (ASCs) (F) and CD24− preadipocytes (G). The percentage of AP cells is shown in each gate (E) (*n* = 4–7 mice for each time point). **H**. Whole-mount images of skin with Bodipy to label neutral lipids and TOPRO3 after a single or three serial depilation. Scale bar is 500μm. **I–J**. Quantification of the area of dermal adipose (I) and number of mature adipocyte (J) in single

or serially depilated skin. (n = 4 mice for each time point). **K**. Flow cytometry plots and quantification of dermal CD24+ adipocyte stem cells (ASCs) (L) and CD24− preadipocytes (M) isolated from single or serially depilated skin. The numbers inside the gates indicate the percentage of AP cells in each gate (K). Statistical analysis was done using One-way ANOVA with Bonferroni post-test for multiple comparisons (B–D and F–G) or Student's T test (I–J and L–M). Data are mean ± SD. Asterisk indicates significance, *p<0.05, **p<0.01, ***p< 0.001 or **** p<0.0001 calculated with One-way ANOVA with Dunnett's or Tukey's post-test for multiple comparisons. See also Figure S2.

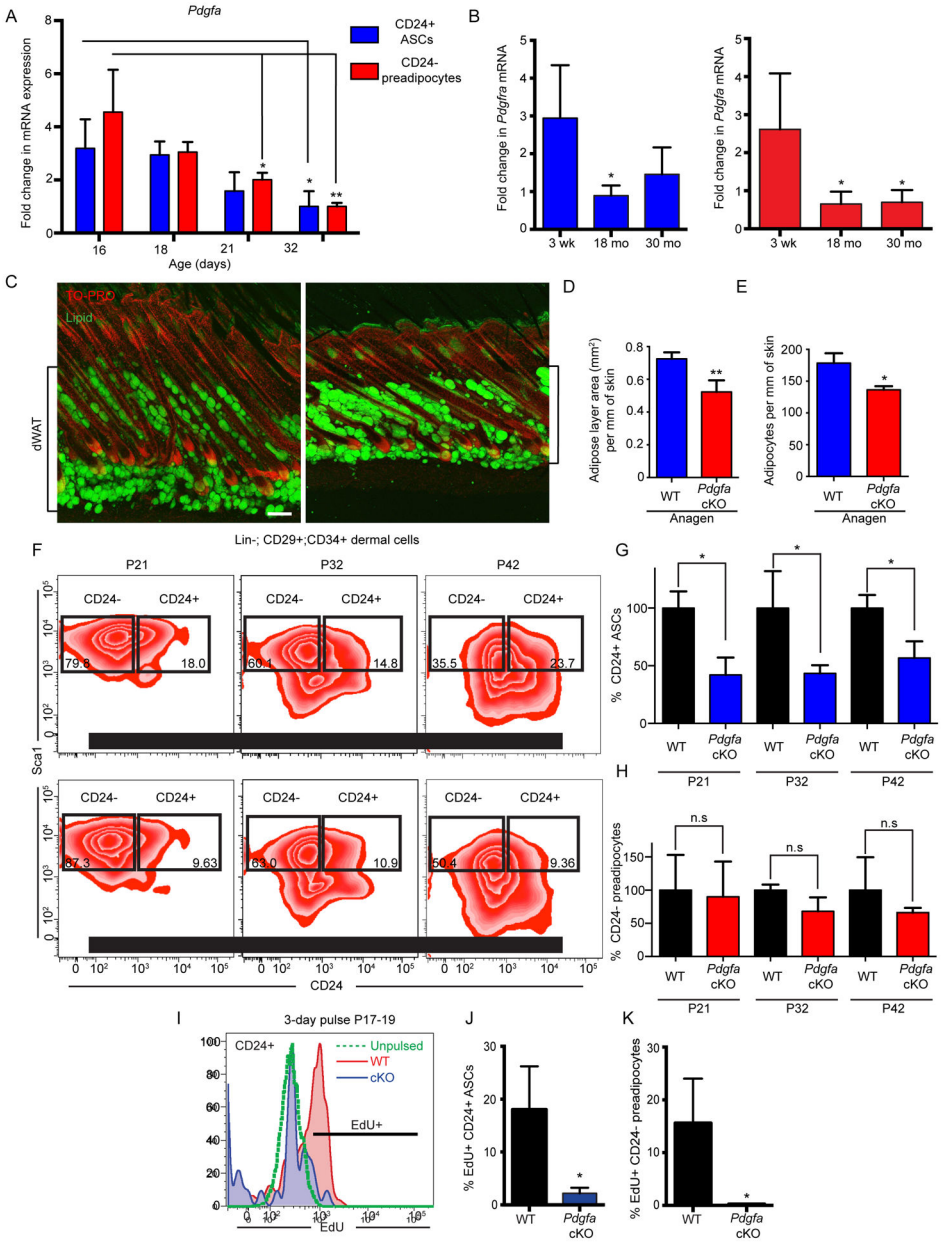

Figure 3. Pdgfa is required for dermal CD24+ ASC and intradermal adipocyte maintenance

A. Real time PCR expression *Pdgfa* mRNA in CD24+ ASCs and CD24− preadipocytes isolated from the skin of mice at indicated ages. Data are mean ± SD normalized to P16 old mice expression levels (n=3–4 mice per group). **B**. *Pdgfa* and *Pdgfrα* mRNA expression in AP cells isolated from WT at 3 weeks, 18 and 30 months of age. Data are mean ± SD normalized to 18 month old mice expression levels (n=3–4 mice per group). **C**. Whole mount confocal images of P32 skin from WT and *Pdgfa* cKO mice stained with Bodipy to label neutral lipids and TOPRO3 to stain nuclei. Scale bar is 200μm. Bracket indicates dermal white adipose (dWAT) thickness. **D**–**E**. Quantification of dermal adipose tissue area (mm^2/mm of skin) (D) and number of mature adipocytes per mm of skin (E) in WT and

Pdgfa cKO mice at age P32. (n=3–4 mice per genotype). **F**. Flow cytometry analysis of APs isolated from skin of WT and *Pdgfa* cKO mice at indicated ages. The percentage of AP cells is indicated in each gate. **G**–**H**. Quantification of CD24+ASCs and CD24− preadipocytes from WT and *Pdgfa* cKO mice at different postnatal days. AP numbers from *Pdgfa* cKO mice are normalized to the WT control in each age group. (n=3 mice per genotype). **I.** Flow cytometry histogram of EdU incorporation in CD24+ ASCs from P20 WT and Pdgfa cKO mice after EdU pulses from P17–19. Control is WT mice without EdU pulse. **J–K** Quantification of the percentage of EdU+ CD24+ adipocyte stem cells (ASCs) (B) or CD24− preadipocytes (C) in WT and *Pdgfa* cKO. (n = 3 mice for each genotype). Data are mean ± SD. Asterisks indicates significance, *p<0.05, **p<0.01, calculated with One-way ANOVA with Dunnett's post-test for multiple comparisons or Student's T test for two groups. See also Figure S3.

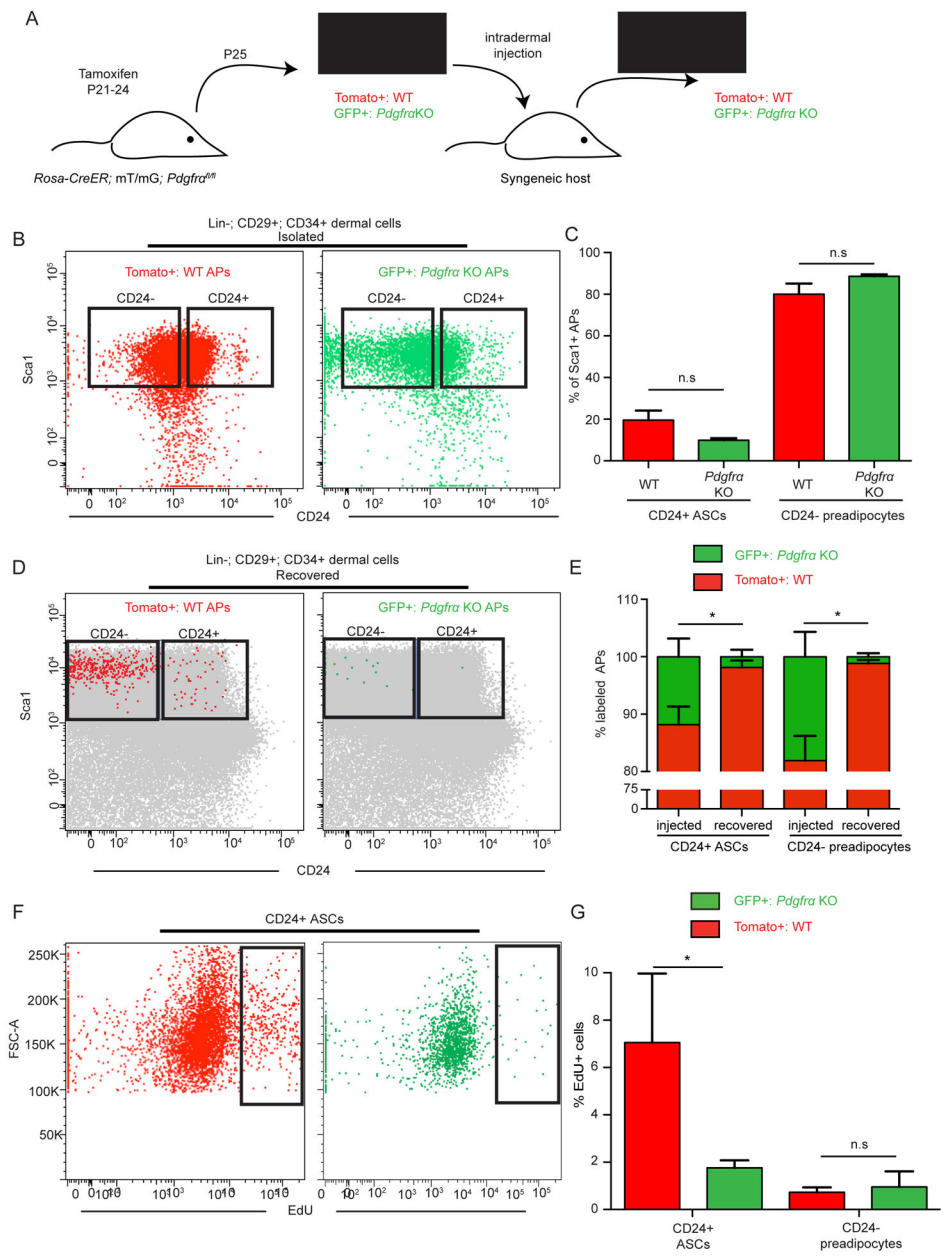

Figure 4. Pdgfr*α* is required for maintenance and proliferation of dermal CD24+ ASCs

A. Schematic of transplantation experiments with Tomato+ (WT) and GFP+ (*Pdgfra* KO) APs from tamoxifen-treated *Rosa*-CreER*;Pdgfra*$^{fl/fl}$ mice into the skin of P15 syngeneic mice. **B–E**. Flow cytometry analysis and quantification of APs isolated from tamoxifen-treated *Rosa*-CreER*;Pdgfra*$^{fl/fl}$ mice (B–C, E) or recovered from host mice 3 days after transplantation (D–E). The dot plot in D shows recovered Tomato+ or GFP+ APs overlaid on WT cells (grey). n=3 mice per genotype (C) or 6 transplant experiments (D). **F–G**. Flow cytometry analysis (F) of EdU incorporation in CD24+ ASCs and quantification in CD24+ ASCs and CD24− preadipocytes (G) from tamoxifen-injected *Rosa-CreER;mTmG;Pdgfra*$^{fl/fl}$ mice after a 6 hr EdU pulse. n=4 mice per genotype. Data are

mean ± SD. Asterisks indicates significance, *p<0.05 calculated with One-way ANOVA with Dunnett's post-test for multiple comparisons. See also Figure S4.

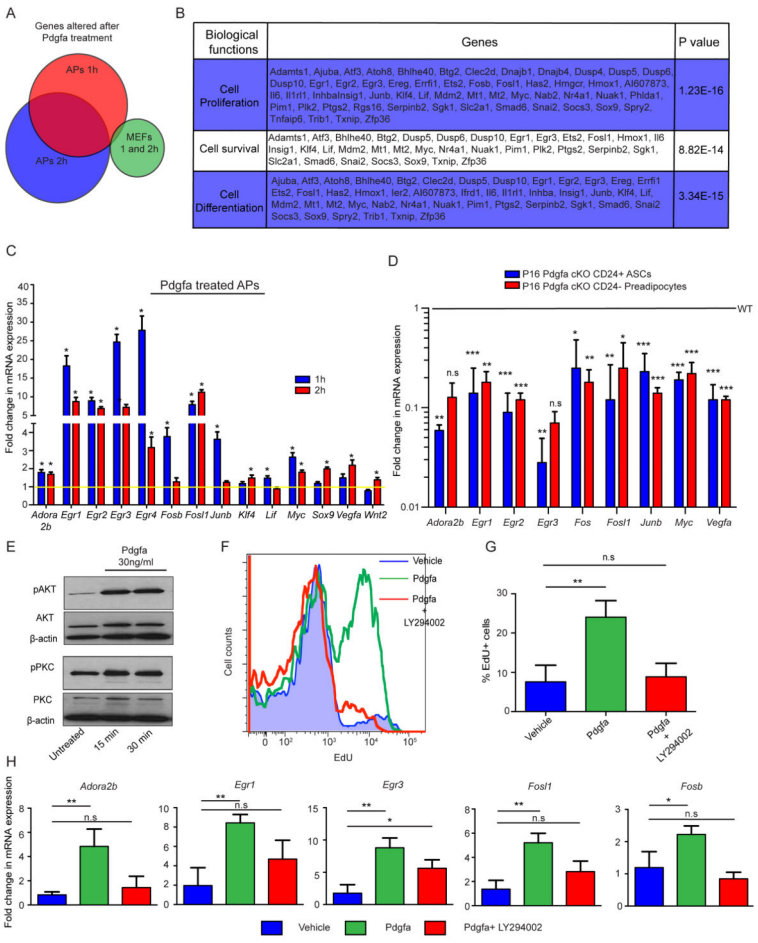

Figure 5. Identification of gene signature induced by Pdgf a in dermal APs

A. Venn diagrams showing overlap between target genes induced by Pdgfa in APs treated with Pdgfa for 1 or 2h or MEFs treated with Pdgfa at similar time points (refs). **B**. Gene ontology (GO) analyses of differentially expressed genes following Pdgfa treatment in APs for 1 and 2 hours. **C**. Real time PCR verification on independently sorted cells confirmed induction with Pdgfa treatment. Data are mean ± SD from 3 measurements. **D**. Pdgfa-target gene expression in CD24+ ASCs and CD24− preadipocytes from P16 WT and *Pdgfa* cKO mice. Gene expression was normalized to WT values. Data are mean ± SD from three biological replicates. **E**. Western blot of phosphorylated Akt (pAkt), Akt, phosphorylated PKC, PKC and β-actin in Pdgfa-treated APs for 15 or 30 min. Representation of 3 independent western blots showing similar results. Flow cytometry analysis (**F**) and quantification (**G**) of EdU incorporation in cultured APs treated with Pdgfa or Pdgfa and LY294002 for 24h. **H**. Real time expression of *Adora2b*, *Egr1*, *Egr3*, *Fosl1* and *Fos* mRNA in cultured APs treated with DMSO and BSA as vehicle, Pdgfa or Pdgfa and LY294002 for 1h. Data are mean ± SD normalized to vehicle treated APs of 3 different AP cultures per treatment. Asterisks indicates significance, *p<0.05, **p<0.01 and ***p< 0.001 calculated with One-way ANOVA with Dunnett's post-test for multiple comparisons. See also Figure S5.

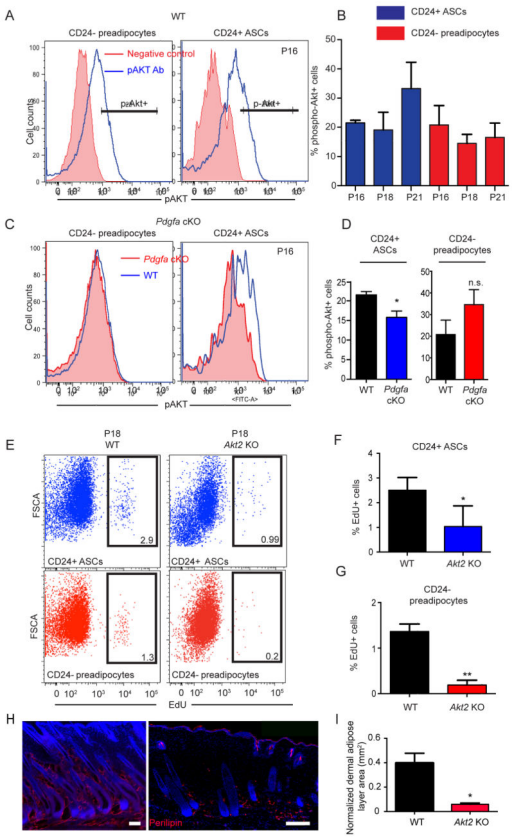

Figure 6. PI3K/Akt pathway is required for dermal AP proliferation

A–D. Flow cytometry histogram plots and quantification of pAKT in WT (A–B) or *Pdgfa* cKO (C–D) CD24+ adipocyte stem cells (ASCs) and CD24− preadipocytes isolated from P16 skin. Data are mean ± SD from 3 mice. **E–G**. Flow cytometry analysis (E) and quantification of EdU incorporation in CD24+ ASCs (F) and CD24− preadipocytes (G) from skin of WT or *Akt2* null mice. Numbers in each gate indicate % of EdU+ cells in each cell type (E). Data are mean ± SD from 3–6 mice. **H–I**. Representative images (H) and quantification (I) of the dWAT in 10–12 week old WT and *Akt2* KO mice. Data are mean ± SD from 3 mice per experimental group. Scale bar is 100μm Statistical analysis were performed using Student's T tests, * $p<0.05$ and ** $p<0.01$. See also Figure S6.